Mediterranean Archaeology and Archaeometry, Vol. 18, No 5, (2018), pp. 147-157

DOI: 10.5281/zenodo.1285897

EXAMINING THE REACTIVITY OF VOLCANIC ASH IN ANCIENT MORTARS BY USING A MICRO-CHEMICAL APPROACH

S. Raneri[1*], S. Pagnotta [1,2], M. Lezzerini[1,2], S. Legnaioli[2], V. Palleschi[2], S. Columbu[3], N.F. Neri[4], P. Mazzoleni[5]

[1]Department of Earth Sciences, University of Pisa, Via S. Maria 53, 56126 Pisa (Italy)
[2]Applied and Laser Spectroscopy Laboratory, Institute of Chemistry of Organometallic Compounds, Research Area of National Research Council, Via G. Moruzzi 1, 56124 Pisa (Italy)
[3]Department of Chemical and Geological Sciences, University of Cagliari, Via Trentino 51, 09127 Cagliari (Italy)
[4]Superintendence for Cultural Heritage of Catania, Via L. Sturzo 62, 95100 Catania (Italy)
[5]Department of Biological, Geological and Environmental Sciences, University of Catania, C.so Italia 57, 95129 Catania (Italy)

Received: 10/11/2017
Accepted: 20/02/2018
**Corresponding author: Simona Raneri (simona.raneri@unipi.it)*

ABSTRACT

A micro-chemical study of ancient mortars has been performed with the aim to evaluate merits and potential of Laser-Induced Breakdown Spectroscopy (LIBS) technique in determining composition of mixtures and evaluating the reactivity of volcanic aggregates, taking advantages from its micro-destructivity and no sample preparation requirements.

LIBS maps have been acquired on areas of about 25 mm^2 on a set of mortars suitable characterised by the occurrence of volcanic rock fragments with a relevant range in grain size. Na, Mg, Al, Si and Ca have been detected and raw maps have been processed using appropriate image processing and statistical methods (*i.e.*: PCA, false colour images, self-organized maps).

The compositional images have been evaluated and interpreted in the light of the supporting data obtained by classical optical microscope and SEM-EDS methods. Results evidenced the possibility to employ LIBS for a preliminary micro-chemical characterization of mortars, revealing also the potentiality of the method to provide compositional and spatial distribution data on aggregate grains and hydraulic phases.

KEYWORDS: micro-LIBS; mortars; chemical maps; reactivity; volcanic ash

1. INTRODUCTION

Chemical analyses on ancient construction materials, often coupled with mineralogical and petrographic studies, are usually included in routine characterization methods finalized to identify raw materials and manufacture processes, and to support restoration procedures in the cultural heritage field (Elsen et al., 2004; Pavía & Caro, 2008; Velosa et al., 2007; Izzo et al., 2016; Liritzis et al., 2015; Hemeda, 2013).

Among cultural materials, mortars stand out for their wide diffusion in buildings and ancient structures, with an outstanding range of functions and manufacture receipts. The characterization of binder and aggregates composition in ancient mortars is often useful to identify the construction phases and to recognize the technologies used in different historical periods (Morricone et al., 2013; Miriello et al., 2010, 2015; Lezzerini et al., 2014, 2017; De Luca et al., 2015; Columbu et al., 2017). Moreover, the possibility to discriminate, on a chemical basis, different features of mortars employed in a certain building, can address information of the possible changes in recipes over the time and over various construction and restoration phases (Gallello et al., 2017).

Apart from binder, aggregates have a key role in determining the final proprieties of mortars; in ancient structures, the choice of aggregates of different nature, shape and grain size were often related to aesthetical vs. practical utility requirements. Since Roman Age, aggregates containing reactive materials were added to lime with the aim of conferring hydraulic character to such mixtures. Natural and artificial reactive aggregates, namely pyroclastic volcanic ash and *cocciopesto*, were mainly employed to achieve this scope (Marra et al. 2011, 2013; Fichera et al., 2015; Columbu & Garau, 2017; Yassen et al., 2013). The activity of volcanic ash in lime mixtures is mainly related to the binder/aggregate ratio, the specific surface of active components able to react, the water content and the environmental curing conditions. Some studies have been recently performed to highlight the influence of volcanic aggregates in carbonation rate (Cultrone et al., 2005) as well the role of aggregates proprieties in reactivity rate (Walker & Pavía, 2011). Generally, higher the fine-grained glassy components of volcanic aggregates is, higher the reactivity is.

The identification of amorphous hydraulic phases is quite easy to achieve by mineralogical, spectroscopic and chemical methods (Paama et al., 1998; Franzini et al., 2000; Elsen, 2006); on the contrary, the visualization and the spatial distribution of hydrate compounds in the mortar matrix in relation to crystalline/glassy reactive aggregates arrangement is less common (Belfiore et al., 2016). Such information appears quite relevant in better understanding the reactive character of different types of natural reactive aggregates such as volcanic ash.

Being able to provide chemical elemental composition of samples without preparation and in very short running time, Laser-Induced Breakdown Spectroscopy (LIBS) technique has been recently proposed for ancient material characterization (Spizzichino & Fantoni, 2014). The method, based on the creation, emission and analysis of a micro-plasma created from a sample surface by a pulsed laser beam, allows detecting and, eventually quantifying, light- and high-Z elements; moreover, thanks to its high spatial resolution, the technique is able to provide elemental maps of a surface. Recent literature has evidenced the drawbacks of the method, the different equipment available for both laboratory and in situ analysis, as well advantages in cultural heritage application (Giakoumaki et al., 2007; Gaudiuso et al., 2010). LIBS has been also tested and successfully employed in natural and artificial stone materials characterization, even by using remote sensing apparatus (Wilsch et al., 2005; Gaona et al., 2013). In mortars studies, LIBS has been demonstrated a useful tool in providing fast, micro-destructive and easy qualitative compositional information about binder and aggregate grains in ancient mortars, giving information also on the textural arrangement of mixtures components (Pagnotta et al., 2017).

To explore potentialities of the method in describing the reactivity of volcanic ash aggregates in ancient mortars, LIBS maps have been acquired on a selection of samples characterized by a wide range of crystalline/glassy texture, grain size and thickening.

Materials have been sampled from a Norman watchtower located in Sicily, namely Adrano Castle (Figure 1), recently interested by restoration works and for which a long debate about construction phases and manufacture techniques in mortar design are still open due to the lack and fragmentary nature of historical information. The interest about the Castle is primary due to its role in the regional territorial control, being part of a wider system of fortification established by Normans to control the Sicilian island, as well to its peculiar aesthetical features, namely the occurrence of covering mortars characterized by volcanic ash aggregates ranging from coarse- to fine-grained.

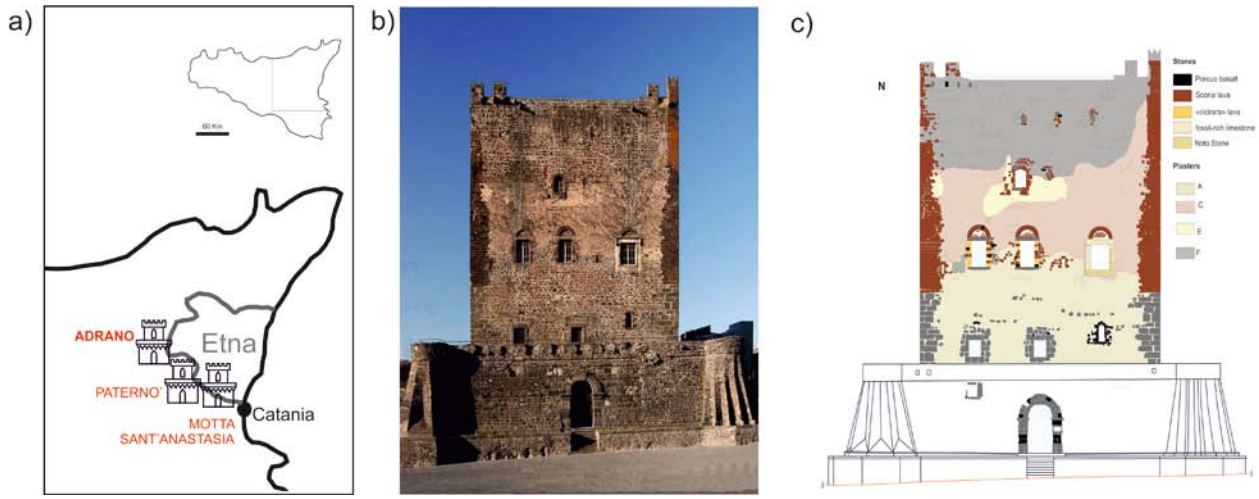

Figure 1. (a) Localization of the site and map of the watchtowers network around Mt. Etna; (b) Picture of the tower; (c) examples of façades mapping from Raneri et al. (2017).

Previous works performed during diagnostic surveys finalized to support restoration works by mapping the façades (Raneri et al., 2017) demonstrated the possible multiple function of such aggregates, including also aesthetical reasons. In fact, samples studied and collected at each of the fourth level of the structure and from the different facing of the tower demonstrated the occurrence of a gradation in grain size of the aggregates from the outer strata to the inner ones.

Both archaeometric aspects, *i.e.* the potential of micro-chemical analysis in mapping and describing reactivity of volcanic aggregates, and methodological ones, *i.e.* the relation between receipts (different grain size and nature of aggregates) and levels of the tower, are the main aims of this study, in which LIBS technique was applied with the support of SEM-EDS and petrographic methods.

The obtained results have been employed to: (i) validate the applied approach in mortars studies, highlighting the possible variation in reactivity degree depending on the grain size of aggregates; (ii) inspect the craftsmen's knowledge related to the different recipes employed over the structure, possibly linked to different construction phases.

2. MATERIALS

The diagnostic study on the materials used to build the Adrano Castle façades have allowed to point out the presence of different mortars, all of them characterized by volcanic sand aggregates with different grain size. A total of 10 stratigraphic units, each of them including three to four levels from the outer strata to the wall blocks, have been sampled from the tower façades. Details about samples and sampling areas are listed in Table 1. Overall, the following mortars can be identified:

- Type A: whitish-grey binder, with lumps and coarse grained volcanic aggregates angular in shape; this mixture occurs mainly on the first two levels of the tower façades, in the outer stratigraphic position;
- Type B: friable and degraded mortar whitish-grey in colour, with medium-fine volcanic aggregates, lumps and low layer cohesion; this mortar occurs irregularly up to the third level of the tower, usually underneath type A mixture;
- Type C: white binder, coarse-grained volcanic aggregates angular in shape, with lumps and medium-high cohesion, identified on all the façades from the lower to the upper levels of the tower, and usually occurring as outward covering mixture;
- Type D: white binder, fine-grained volcanic aggregates, rare *cocciopesto*, medium-high cohesion and discontinuously covered by a pale-red plaster, distributed along all the façades, underneath type C;
- Type E: white binder plaster resembling type D, but in a different stratigraphic position and characterized by coarser-grained inclusions;
- Type F: heterogeneous grey binder characterized by high cohesion, quartz sand aggregates and volcanic coarse-grained aggregates, not systematically covered by a pale-red coloured layer and occurring especially from the third tower level on all the façades.

Table 1. Macroscopic features of mortar samples. The alphanumeric name of the samples accounts a letter indicating the facing, a Roman number indicating the level and an Arab number indicating the stratigraphic position (from outer to inner strata).

Façade	Level Tower floor	Sample ID[1]	Binder Colour	Aggregates		Cohesion	Type
				Grain size	Thickening		
North facing	I	N-I-1	whitish-grey	coarse to medium	high	friable	A
		N-I-2	whitish-grey	medium to fine	medium-low	friable	B
	II	N-II-1	gray	coarse to medium	high	very tough	F
		N-II-2	white	medium to fine	medium-low	tenacious	D
		N-II-3	white	coarse to medium	high	tenacious	C
		N-II-4	whitish-grey	medium to fine	medium-low	friable	B
	III	N-III-1	grey	coarse to medium	high	very tough	F
		N-III-2	white	medium to fine	medium-low	tenacious	E
		N-III-3	white	coarse to medium	high	tenacious	C
		N-III-4	white	medium to fine	medium-low	tenacious	D
	IV	N-IV-1	grey	coarse to medium	high	very tough	F
		N-IV-2	white	coarse to medium	high	tenacious	C
South facing	II	S-II-1	whitish-grey	coarse to medium	high	friable	A
		S-II-2	white	medium to fine	medium-low	tenacious	D
		S-II-3	whitish-grey	medium to fine	medium-low	friable	B
	III	S-III-1	gray	coarse to medium	high	very tough	F
		S-III-2	white	coarse to medium	high	tenacious	C
		S-III-3	whitish-grey	medium to fine	medium-low	friable	B
		S-III-4	white	medium to fine	medium-low	tenacious	D
West facing	II	O-II-1	white	medium to fine	medium-low	tenacious	D
		O-II-2	grey	coarse to medium	high	very tough	F
		O-II-3	white	coarse to medium	high	tenacious	C
		O-II-4	grey	coarse to medium	high	very tough	F
	III	O-III-1	grey	coarse to medium	high	very tough	F
		O-III-2	white	coarse to medium	high	tenacious	C
		O-III-3	white	medium to fine	medium-low	tenacious	E
		O-III-4	white	coarse to medium	high	tenacious	C
East facing	II	E-II-1	grey	coarse to medium	high	very tough	F
		E-II-2	whitish-grey	coarse to medium	high	friable	A
		E-II-3	whitish-grey	medium to fine	medium-low	friable	B
	III	E-III-1a	whitish-grey	coarse to medium	high	friable	A
		E-III-2a	white	coarse to medium	medium-low	tenacious	C
		E-III-3a	white	medium to fine	medium-low	tenacious	D
		E-III-1b	white	coarse to medium	medium-low	tenacious	C
		E-III-2b	white	medium to fine	medium-low	tenacious	D
		E-III-3b	white	medium to fine	medium-low	tenacious	D
		E-IV-4b	white	medium to fine	medium-low	tenacious	E

3. EXPERIMENTAL

Micro-LIBS setup based on a Modì double-pulse instrument has been employed for acquiring chemical maps on small pieces remaining from thin section preparation. In the instrument, the laser pulse is sent through the Modì articulated arm into a Zeiss Axio microscope, and then focused onto the sample. The use of a double-pulse system for LIBS micro-analysis has been proven suitable for the analysis of mortars (Pagnotta et al., 2017). The typical diameter of the craters produced is around 20 μm, using a 5+5 mJ energy of the laser pulses (about 20 ns FWHM). The delay between the pulses was set at 1 μs. The LIBS signal was collected by an optical fibre, placed at 45 degrees with respect to the laser direction, at a distance of about 1 cm from the sample; a ball lens in front of the fibre guarantees the optimal collection of the LIBS signal from the whole plasma. The Modì instrument uses an Avantes double spectrometer (AvaSpec-2048-2), which covers the spectral region from 190 to 900 nm (0.1 nm resolution from 190 to 450 nm, 0.3 nm resolution from 450 to 900 nm). The element maps were acquired on a 50x50 matrix (2500 LIBS spectra) with a lateral resolution of 100 μm for a total scanned area of 25 mm^2. The elements mapped on the mortar's surface are reported in Table 2, along with the central wavelength of the emission line used.

Table 2 Elements mapped and central wavelength of the emission line.

Element	λ (nm)
Na	589.0
Mg	279.6
Al	309.3
Si	288.2
Ca	393.4

Although the LIBS technique would allow a quantitative determination of the elemental composition of the sample (Tognoni et al., 2002), the analysis has been limited to the qualitative mapping of the binder and aggregate compositions. Chemical maps obtained by LIBS have been processed by using statistical and image processing methods.

The mortar characterization has been complemented by the support case of Earth Sciences classical methodologies; in detail, Optical Microscopy (OM) and Scanning Electron Microscopy equipped with an Energy-dispersive X-ray Spectroscopy apparatus (SEM-EDS) have been employed to characterize representative samples for each type of mortar sampled from façades and tower levels. In details, mineralogical and petrographic investigations have been carried out on polished thin sections by using a Carl Zeiss Axioplan polarizing microscope. Scanning electron microscope observations and microchemical compositions of aggregates, lumps and intergranular binders have been performed using a Philips XL30 instrument equipped with an energy dispersive spectrometer EDAX (standardless software DXi4) with 20 kV acceleration voltage, 0.1 nA beam current, and 100 s live time.

4. RESULTS

4.1. *Preliminary mineralogical and petrographic characterization*

With the aim to support the applied experimental micro-chemical approach, thin section analysis has been carried out on samples representative of the different mortars identified by macroscopic observations. From the petrographic point of view, the studied mortar samples exhibit different textures and a quite relevant range in binder/aggregate ratio, as well as in the morphological and morphometric distribution of aggregates (Figure 2). In detail, the thin section analysis allowed discriminating five groups (types A-F). Aggregate/binder ratio ranges from 3:1 (in types A, C and F) to 1:3 (in B, D and E); the binder is from inhomogeneous and greyish in color (in types A and B) to white in color with abundant lumps (in types C, D and E). A different appearance can be assessed for type F, which is distinguished from the other groups for the occurrence of quartz sandy aggregates and a not homogenous and dark grey binder. The percentage of voids, visually esteemed by microscopy, ranges from 10 to 20 vol% and consists in primary (capillary voids and shrinkage cracks) and secondary porosity (due to dissolution).

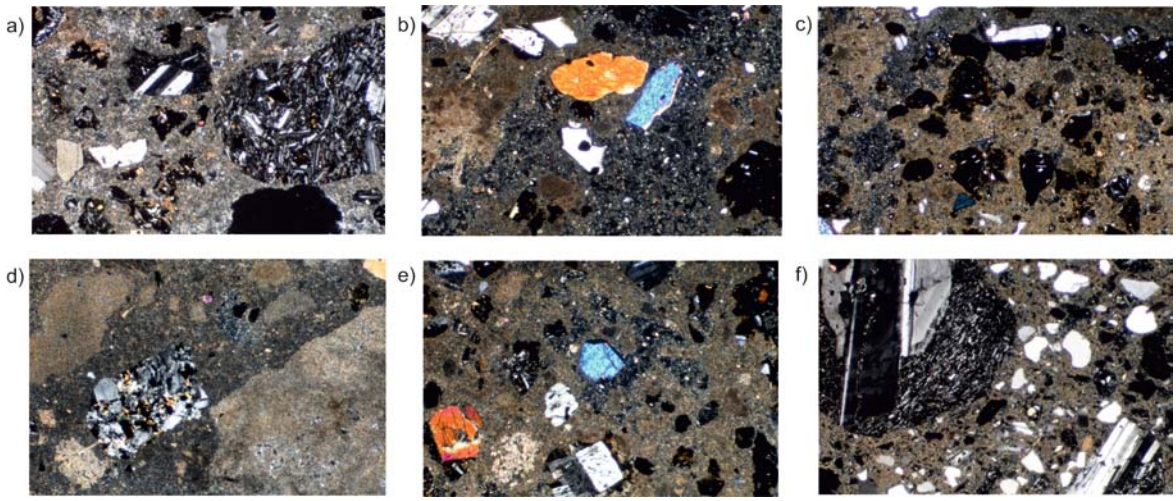

Figure 2. Thin sections of representative samples of the different mortars (the long side of the pictures is 3.2 mm long; crossed polarised ligh): (a) Type A, sample N-I-1, (whitish-grey binder, with lumps and coarse grained volcanic aggregates angular in shape, high thickening); (b) Type B, sample S-II-3, (white binder, medium-fine volcanic aggregates, abundant lumps, low thickening); (c) Type C, sample S-III-2, (white binder, coarse grained volcanic aggregates, with rare lumps, low thickening); (d) Type D, sample N-II-2, (white binder, fine-grained volcanic aggregates, very low thickening, rare cocciopesto); (e) Type E, sample O-III-3, (white binder plaster resembling type D, low thickening); (f) Type F, sample N-II-1, (not homogeneous dark grey binder plaster with quartz sandy aggregates and volcanic coarse-grained aggregates).

As regards aggregates, they consist of volcanic rock fragments (plagioclases and pyroxenes, plus amorphous phases) ranging from crystalline texture, typical of Etna basaltic lavas, to cryptocrystalline one, even glassy. From the compositional point of view, binders seem due to calcite + CSH phases, probably obtained by adding fine-grained reactive volcanic ash; actually, in some cases, reaction rims have been observed related to glassy aggregates.

4.2. *μ-LIBS maps*

In spite of the numerous information achievable by μ-LIBS method, the interpretation of the maps is not straightforward; the inspection of elemental maps might allow evidencing the distribution of aggregate grains, as well possible differences in mineralogical composition of both binders and aggregates. Moreover, in the present case study, the occurrence of reaction rims and hydraulic phases could be pointed out by the presence of Si-Al-rich areas in respect to the calcite-based binder**.** False color maps might contribute to qualitatively describe chemical composition of mixtures. In maps of Figure 3, red channel accounts Si contribute, while blue and green channels describe Ca and Al contents, respectively. Based on a qualitative evaluation, it is possible to state that studied mixtures exhibit a quite similar composition, with false color maps exhibiting more or less intense shades of magenta. Exception it is sample N-II-1 (type F) in which orange-light red areas are prevalent; effectively, the occurrence of quartz aggregates evidenced by thin section observation turns in higher red channel intensity in false color maps respect to other mixtures.

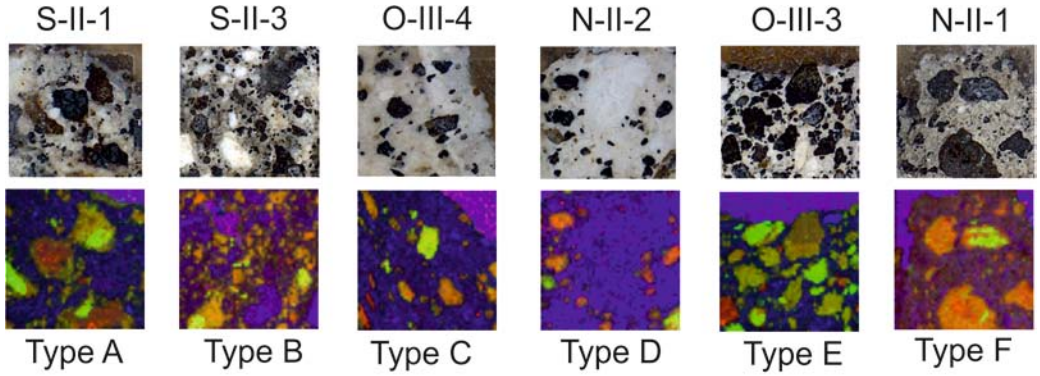

Figure 3. Macrophotos and false-colours RGB maps (side of pictures 5 mm) of Si (red), Al (green) and Ca (blue) distribution in the analysed samples.

However, the interpretative problems due to limits occurring also in other multispectral-based techniques, concerning for example the representation of different bands in only one map, have to be taken in account. In this perspective, image processing and statistical methods can greatly improve results and interpretations.

For example, considering the ratio between two elements, the possible homogeneity/not homogeneity of the binder can be pointed out. In Figure 4a, Ca/Mg ratio maps for mortar samples representative of the studied mixture types are reported; effectively, some differences among samples can be highlighted, revealing the minimum ratio level for mixtures A, C and E.

Of course, a more comprehensive chemical characterization of samples requires the analysis of all detected elements; for this reason, Principal Component Analysis (PCA) has been also applied to the acquired images (Jolliffe, 1986; Wold et al., 1987). Maps obtained by using this approach might provide information about the average composition of the mixtures, highlighting also possible differences in aggregate grains and/or binder composition.

On the basis of PCA images (Figure 4b) the following considerations can be provided. As regards aggregates, as expected, they are clearly separated from the binders due to their quite homogenous composition along the studied mixtures. Moreover, maps reveal useful information about morphology and grain aggregates distribution, providing insights on thickening and shape, the latter one possibly related to the crystalline vs. glassy texture of volcanic rock fragments (the first sharper than the latter ones, exhibiting irregular edges). Concerning binder, the ranging in color (from light blue to deep green) is coherent with the previously observed variability based on calcium and magnesium level, even if the possible contribute of silica and alumina have to be considered.

A better visualization of chemical maps can be achieved by Self-Organizing Maps (SOM) method, known also as the Kohonen Maps method after the name of its inventor (Kohonen, 1990). The SOM method is extremely useful, among other applica-

tions, for the automatic segmentation of digital imaging, *i.e.* for the separation of areas characterized by different signatures. In our applications, the signature corresponds to the elemental composition of the binder and the aggregates in the mortars. The SOM method assigns the image pixels to the closest neuron, in a n-dimension space, where n corresponds to the number of elements considered (8, in our case). The eight coordinates of the winning neurons can be considered as the coordinates of the centroid of the cluster or, which is the same to say, as the average composition of the members of the cluster. The SOM method has the advantage, with respect to other methods as the K-means segmentation (Ng et al., 2006), for example, of not requiring an a priori knowledge of the number of clusters. Moreover, the SOM method does not make use of any dimensional reduction for being effective.

The processed SOM maps for the studied mortars are reported in Figure 4c. The analysis of the images might be useful to highlight the possible reactions between binders and aggregates**, the latter ones turning in light areas or dense dotted areas (green plus blue channels or green plus red channels) in function of qualitative compositional variability of the mixtures**. Effectively, red-purple rims are quite evident along the edge of some clasts of aggregate**s**, particularly in relation to irregular in shape fragments of glassy material.

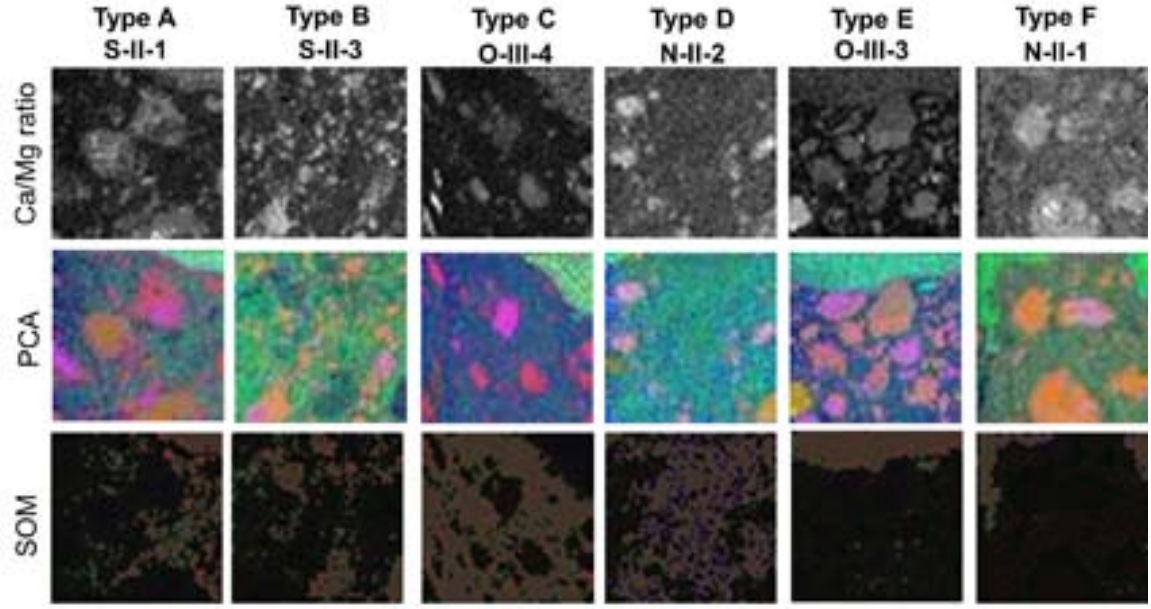

Figure 4. Micro-LIBS maps (side of pictures 5 mm) acquired on representative samples for each identified mortar type. (top images) Elemental maps Ca/Mg ratio: the zero intensity (black) corresponds to the minimum peak intensity of the ratio, while intensity 255 (white) corresponds to its maximum. (central images) PCA maps (false-color) evaluated on the relative abundance of the following elements Na, Mg, Al, Si, Ca. (bottom images) SOM maps.

4.3. SEM-EDS chemical data

In order to support the results obtained by LIBS and critically evaluate the merits of the method in mortar studies, SEM-EDS analysis have been performed on samples previously inspected by micro-LIBS. Chemical data have been thus employed to determine the chemical composition of studied materials, trying to correlate the possible different reactivity level of volcanic sand in the mixtures in function of grain size and thickening, as well to compare data with micro-LIBS maps. For this purpose, chemical data collected on lumps, intergranular binders and aggregates have been plotted in the ternary diagrams $CaO+MgO-Al_2O_3-SiO_2$ (Fig. 5, Table 3).

Table 3. Average chemical EDS data (wt%) and standard deviation collected on lumps, intergranular binders and aggregates in samples representative of the different mortar types.

Type	Analysed fraction	Na_2O	MgO	Al_2O_3	SiO_2	P_2O_5	S	K_2O	CaO	TiO_2	MnO	Fe_2O_3	CaO+MgO	SiO_2+Al_2O_3+Fe_2O_3	HI
A	lumps	0.19	2.53	0.87	4.19	<0,01	0.34	0.50	90.89	<0,01	<0,01	0.42	93.42	5.49	0.06
		0.22	1.23	0.33	2.80	-	0.09	0.35	5.19	-	-	0.26			
	intergranular binder	0.54	3.34	3.22	11.38	<0,01	0.82	0.34	76.10	0.28	1.00	3.33	79.44	17.93	0.23
		0.76	1.57	0.30	5.70	-	0.39	0.18	13.57	0.08	0.28	0.84			
	aggregates	2.81	3.52	20.55	54.08	<0,01	<0,01	2.02	12.99	<0,01	<0,01	3.79			
		1.64	1.80	8.44	5.33	-	-	1.01	5.89	-	-	0.98			
B	lumps	0.04	5.24	0.11	3.04	<0,01	<0,01	0.05	90.71	<0,01	0.04	0.95	95.95	4.10	0.04
		0.02	0.08	0.02	0.02	-	-	0.02	0.11	-	0.01				
	intergranular binder	0.44	5.92	1.18	5.54	<0,01	0.37	0.15	84.81	<0,01	0.54	0.92	90.74	7.64	0.08
		0.18	1.91	1.51	0.73	-	0.18	0.03	6.05	-	0.39	0.50			
	aggregates	4.18	2.92	22.05	52.80	<0,01	<0,01	1.24	11.49	0.99	0.23	4.32			
		1.72	0.97	8.62	3.62	-	-	0.20	4.91	0.75	0.30	0.49			
C	lumps	1.02	5.48	2.32	1.01	<0,01	<0,01	0.76	87.71	<0,01	0.59	0.72	93.19	4.05	0.04
		0.34	1.57	0.30	0.27	-	-	0.33	2.41	-	0.17	0.30			
	intergranular binder	0.36	3.47	2.48	10.03	<0,01	<0,01	0.99	80.62	0.47	0.44	0.91	84.09	13.42	0.16
		0.72	1.51	1.46	3.33	-	-	0.17	6.21	0.75	0.33	0.13			
	aggregates	3.47	1.82	26.10	50.93	<0,01	<0,01	1.08	11.40	<0,01	<0,01	5.19			
		0.49	0.15	9.32	1.98	-	-	0.11	4.58	-	-	1.21			
D	lumps	0.74	3.84	2.39	0.94	0.49	0.40	0.18	89.42	0.39	0.70	0.56	93.26	3.88	0.04
		0.18	1.47	0.64	0.14	0.20	0.13	0.02	3.30	0.07	0.09	0.06			
	intergranular binder	2.01	5.74	3.78	5.66	0.45	0.79	0.35	78.60	0.69	0.78	1.09	84.35	10.52	0.12
		0.84	2.66	1.65	2.73	0.03	0.03	0.04	7.89	0.10	0.54	0.74			
	aggregates	1.80	0.67	27.41	51.44	<0,01	<0,01	0.55	14.00	0.66	<0,01	3.48			
		2.17	1.25	5.69	1.93	-	-	0.18	2.20	0.15		1.46			
E	lump	<0,01	1.71	0.84	3.55	0.50	0.54	<0,01	90.79	1.01	<0,01	0.66	92.50	5.05	0.05
		-	0.53	0.25	0.64	0.01	0.01	-	4.38	0.15	-	0.09			
	intergranular binder	0.96	5.18	3.91	7.22	0.65	1.28	0.41	79.29	<0,01	<0,01	1.20	84.47	12.33	0.15
		0.07	1.24	0.56	1.23	0.03	0.10	0.05	1.98	-	-	0.05			
	aggregates	3.11	2.33	22.32	41.45	<0,01	<0,01	<0,01	9.93	1.67	<0,01	19.88			
		1.46	1.32	9.91	23.33	-	-	-	5.56	0.51	-	5.18			
F	lump	0.65	2.11	1.70	0.77	<0,01	<0,01	0.75	93.36	<0,01	<0,01	0.33	95.47	2.80	0.03
		0.01	0.16	0.22	0.06	-	-	0.01	3.72	-	-	0.01			
	intergranular binder	0.34	2.73	2.99	5.47	<0,01	0.61	0.96	85.45	0.21	<0,01	1.08	88.19	9.53	0.11
		0.30	0.99	1.11	1.13		0.27	0.09	2.32	0.18	-	0.16			
	aggregates	1.99	2.63	13.78	32.87	0.21	<0,01	1.66	40.82	0.90	<0,01	5.26			
		1.02	2.31	10.40	25.41	0.33		1.02	38.37	1.14	-	4.90			

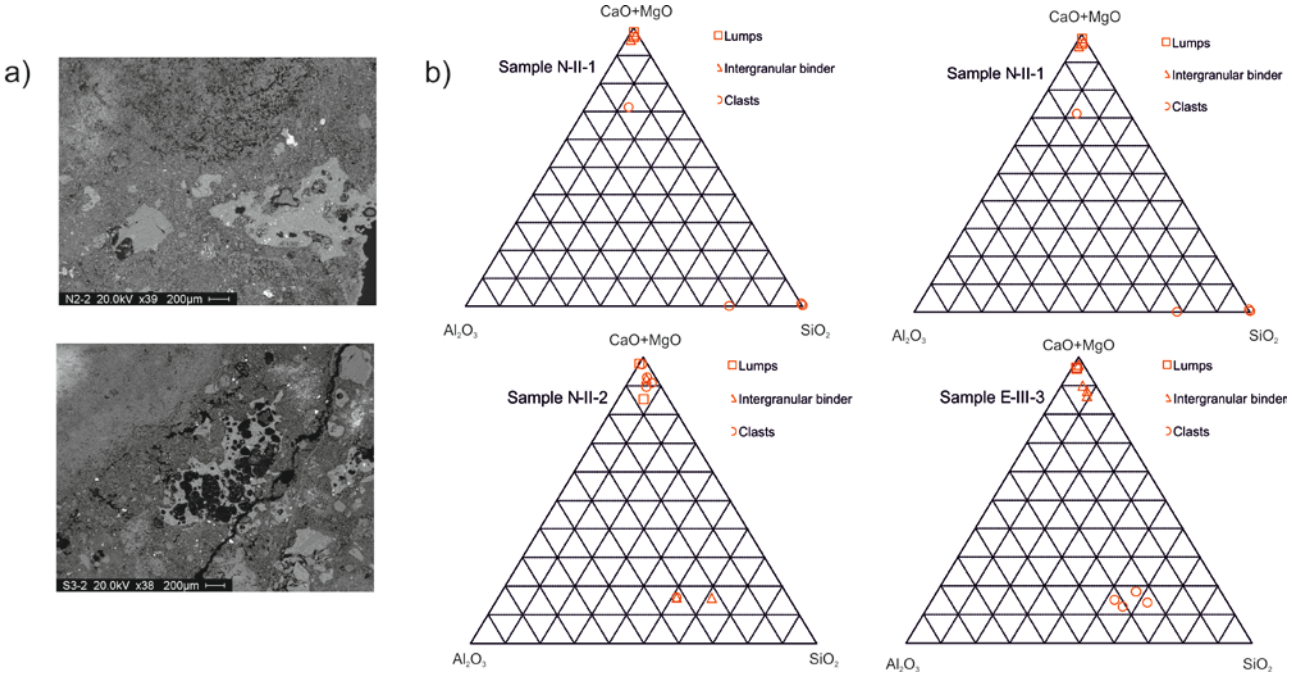

Figure 5. (a) SEM images as examples of lumps, intergranular binder and glassy aggregates in some studied mortars; (b) Ternary diagrams CaO+MgO-Al_2O_3-SiO_2.

Concerning interaction between binder and aggregates, obtained data suggest that volcanic aggregates are partially responsible of the hydraulic character of the binder, as suggested by the plot of intergranular binder composition in ternary diagrams. Moreover, a more careful inspection of diagrams reveals that slight differences can be observed among studied mortar mixture types. Generally, as expected, the finer the aggregate is, the more hydraulic the binder is; on the contrary, thickening seems do not play a relevant role in the determined reactivity levels.

5. DISCUSSION AND CONCLUSIONS

In reviewing the merits of micro-LIBS in the proposed application, the following consideration can be summarised. Firstly, micro-LIBS maps provided useful information about aggregate grains, including

their spatial distribution and shape. In the matter in question, the possibility to evaluate aggregate grain size and discriminate rock fragments (with sharp morphology) and volcanic glassy fragments (more irregular) can offer insights on the manufacture process as well on the effective contribute of reactive silicates and aluminates to the hydraulic character of the mixtures. Secondly, as regard the mortar binder, the Ca/Mg ratio maps revealed the occurrence of slight differences among studied samples in regards to calcium and magnesium relative abundance, as evidenced also by SEM-EDS analysis. The application of PCA processing method enlarged the compositional evaluation of studied materials, allowing discriminate homogenous and not quite homogenous mixtures on the basis of the green vs. blue areas arrangement. Trying to correlate the false colour distribution to the chemical composition, SEM-EDS data have been employed to calculate HI index of intergranular binder (HI = $(SiO_2+Al_2O_3+Fe_2O_3)/(CaO+MgO)$) and results (Fig. 6) have been compared with PCA maps. With values ranging from 0.08 to about 2, samples exhibiting the lower HI values (types B, D and F) show PCA maps characterised by green-light green false colour areas, while in mortars characterised by a more hydraulic character the binder appears deep blue in colour (types A, C and E). According to these experimental evidences, we can hypothesise a correlation between HI and false colour PCA maps, even if the absence of iron in PCA calculation has to be taken in account.

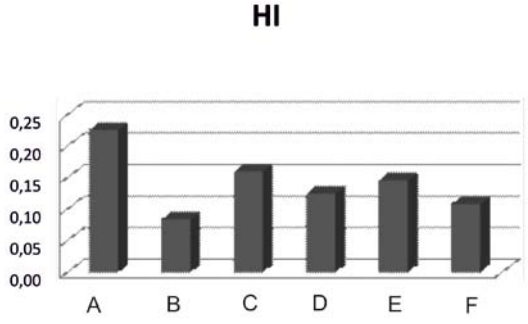

Figure 6. HI values calculated for each mortar type on the basis of SEM-EDS data.

Thirdly, going to inspect the possible correlation between reactivity level and grain size of aggregates, we can state that no strictly relationship was evidenced by both LIBS and SEM-EDS analyses. On the whole, the constructed triangular diagrams suggested a slightly more reactive behaviour in samples with fine-medium grained aggregates (for example in mixture types D and C); these data are weakly correlated with SOM maps, even if the latter ones help to identify reaction rims at glassy fragments edges, informing us about the spatial distribution of hydraulic phases.

Finally, the overall obtained results not evidenced a strict relation among spatial distribution and reactivity level of volcanic aggregates, neither a systematic association between the compositional variability and the stratigraphy of covering mortars, suggesting that the occurrence of different mixtures has to be related to subsequent interventions on the tower, operated by different artisans and workshops. Thus, we can hypothesise that even if fine-grained volcanic ash were probably added to confer hydraulic character to the mixtures, the ranging in grain size evidenced by macro and microscopic observations meet more credibly aesthetical requirements, kept unaltered over the time and over the building levels.

Concluding, following the main aim of the research, namely validate LIBS in micro-chemical studies on ancient mortars and particularly in obtaining spatial distribution and chemical related data, we can finally state that the method is suitable to study aggregates grain features and obtain qualitative information on the hydraulic character of mortars, supported by spatial arrangement information. Obtained data appears in good agreement with SEM-EDS results, suggesting the method as adequate enough for rapid and preliminary characterization of artificial stone materials with a micro-destructive and not too time-consuming approach. Of course, to include micro-LIBS mapping in routine methods for mortar studies, a larger set of materials should be systematically investigated, trying also to go behind the merely qualitative approach and evaluating the possibility to extract quantitative data.

ACKNOWLEDGEMENTS

We thank the Superintendence for Cultural Heritage of Catania for having allowed the sampling campaign of the studied covering mortars during the restoration works started in 2015 at the Adrano Castle (Adrano, Catania, Sicily).

REFERENCES

Belfiore, C. M., Fichera, G.V., Ortolano, G., Pezzino, A., Visalli, R., Zappalà, L. (2016) Image processing of the pozzolanic reactions in Roman mortars via X-Ray Map Analyser. *Microchemical Journal*, Vol. 125, pp. 242-253.

Columbu S., Garau A.M. (2017) Mineralogical, petrographic and chemical analysis of geomaterials used in the mortars of Roman Nora theatre (south Sardinia, Italy). *Italian Journal of Geosciences*, Vol. 136, pp. 238-262.

Columbu S., Sitzia F., Ennas G. (2017) The ancient pozzolanic mortars and concretes of Heliocaminus baths in Hadrian's Villa (Tivoli, Italy). *Archaeological and Anthropological Sciences*, Vol. 9, pp. 523-553.

Cultrone, G., Sebastián, E., Ortega Huertas, M. (2005) Forced and natural carbonation of lime-based mortars with and without additives: Mineralogical and textural changes. *Cement and Concrete Research*, Vol. 35, No 12, pp. 2278-2289.

De Luca, R., Miriello, D., Pecci, A., Domínguez-Bella, S., Bernal-Casasola, D., Cottica, D., Bloise, A., Crisci, G.M. (2015) Archaeometric Study of Mortars from the Garum Shop at Pompeii, Campania, Italy. *Geoarchaeology*, Vol. 30, No 4, pp. 330-351.

Elsen, J. (2006) Microscopy of historic mortars—a review. *Cement and Concrete Research*, Vol. 36, No 8, pp. 1416-1424.

Elsen, J., Brutsaert, A., Deckers, M., Brulet, R. (2004) Microscopical study of ancient mortars from Tournai (Belgium). *Materials Characterization*, Vol. 53, No 2–4, pp. 289-294.

Fichera, G.V., Belfiore, C.M., La Russa, M.F., Ruffolo, S.A., Barca, D., Frontoni, R., Galli, G., Pezzino, A. (**2015**) Limestone Provenance in Roman Lime-Volcanic Ash Mortars from the Villa Dei Quintili, Rome. *Geoarchaeology*, Vol. 30, No 2, pp. 79–99.

Franzini, M., Leoni, L., Lezzerini, M. (2000) A procedure for determining the chemical composition of binder and aggregate in ancient mortars: its application to mortars from some medieval buildings in Pisa. *Journal of Cultural Heritage*, Vol. 1, No 4, pp. 365-373.

Gallello, G., Ramacciotti, M., Lezzerini, M., Hernandez, E., Calvo, M., Morales, A., Pastor, A., de la Guardia, M. (2017) Indirect chronology method employing rare earth elements to identify Sagunto Castle mortar construction periods. *Microchemical Journal*, Vol. 132, pp. 251-261.

Gaona, I., Lucena, P., Moros, J., Fortes, F. J., Guirado, S., Serrano, J., Laserna, J. J. (2013) Evaluating the use of standoff LIBS in architectural heritage: surveying the Cathedral of Málaga. *Journal of Analytical Atomic Spectrometry*, Vol. 28, pp. 810-820.

Gaudiuso, R., Dell'Aglio, M., De Pascale, O., Senesi, G.O., De Giacomo, A. (2010) Laser Induced Breakdown Spectroscopy for Elemental Analysis in Environmental, Cultural Heritage and Space Applications: A Review of Methods and Results. *Sensors*, Vol. 10, pp. 7434-7468.

Giakoumaki, A., Melessanaki, K., Anglos, D. (2007) Laser-induced breakdown spectroscopy (LIBS) in archaeological science—applications and prospects. *Analytical and Bioanalytical Chemistry*, Vol. 387, No 3, pp. 749–760.

Hemeda, S (2013) Laser induced breakdown spectroscopy and other analytical techniques applied on construction materials at Kom el-Dikka, Alexandria, Egypt. *Mediterranean Archaeology and Archaeometry*, Vol. 13, No 2, pp. 103-119

Izzo, F., Arizzi, A., Cappelletti, P., Cultrone, G., De Bonis, A., Germinario, C., Graziano, S.F., Grifa, C., Guarino, V., Mercurio, M., Morra, V., Langella, A. (2016) The art of building in the Roman period (89 B.C. – 79 A.D.): Mortars, plasters and mosaic floors from ancient Stabiae (Naples, Italy). *Construction and Building Materials*, Vol. 117, pp. 129-143.

Jolliffe, I. T. (1986) *Principal Component Analysis and Factor Analysis*. In Principal component analysis. Springer, pp. 115–128.

Kohonen, T. (1990) The self-organizing map. *Proceedings of the IEEE*, 78(9), pp. 1464–1480.

Lezzerini, M., Legnaioli, S., Lorenzetti, G., Palleschi, V., Tamponi, M. (2014) Characterization of historical mortars from the bell tower of St. Nicholas church (Pisa, Italy). *Construction and Building Materials*, Vol. 69, pp. 203-212.

Lezzerini, M., Ramacciotti M., Cantini F., Fatighenti B., Antonelli F., Pecchioni E., Fratini F., Cantisani E., Giamello, M. (2017) Archaeometric study of natural hydraulic mortars: the case of the Late Roman Villa dell'Oratorio (Florence, Italy). *Archaeological and Anthropological Sciences*, Vol. 9, pp. 603-615.

Liritzis, I, Al-Otaibi, F, Kilikoglou, V, Perdikatsis, V, Polychroniadou, E, Drivaliari, A (2015) Mortar analysis of wall painting at Amfissa Cathedral for conservation-restoration purposes. *Mediterranean Archaeology and Archaeometry*, Vol. 15, No 3, pp. 301-311 (DOI: 10.5281/zenodo.33833).

Marra, F., D'Ambrosio, E., Sottili, G., Ventura, G. (2013) Geochemical Fingerprints of Volcanic Materials: Identification of a Pumice Trade Route from Pompeii to Rome. *Geological Society of America Bulletin*, Vol. 125, No 3–4, pp. 556–77.

Marra, F., Deocampo, D., Jackson, M.D., Ventura, G. (2011) The Alban Hills and Monti Sabatini Volcanic Products Used in Ancient Roman Masonry (Italy): An Integrated Stratigraphic, Archaeological, Environmental and Geochemical Approach. *Earth-Science Reviews*, Vol. 108, No. 3–4, pp. 115–36.

Miriello D., Antonelli F., Apollaro C., Bloise A., Bruno N., Catalano E., Columbu S., Crisci G.M., De Luca R., Lezzerini M., Mancuso S., La Marca A. (2015) New data about the ancient mortars from the archaeological site of Kyme (Turkey): compositional characterization. *Periodico di Mineralogia*, Vol. 84, No. 3A, pp. 497–517.

Miriello, D., Barca, D., Bloise, A., Ciarallo, A., Crisci, G.M., De Rose, T., Gattuso, C., Gazineo, F., La Russa, M.F. (2010) Characterisation of archaeological mortars from Pompeii (Campania, Italy) and identification of construction phases by compositional data analysis. *Journal of Archaeological Science*, Vol. 37, No. 9, pp. 2207-2223.

Morricone, A., Macchia, A., Campanella, L., David, M., De Togni, S., Turci, M., Maras, A., Meucci, C., Ronca, S. (2013) Archaeometrical analysis for the characterization of mortars from Ostia Antica. *Procedia Chemistry*, Vol. 8, pp. 231-238.

Ng, H. P., Ong, S. H., Foong, K. W. C., Goh, P. S., & Nowinski, W. L. (2006). Medical image segmentation using k-means clustering and improved watershed algorithm. In *Image Analysis and Interpretation, 2006 IEEE Southwest Symposium on* (pp. 61–65). IEEE.

Paama, L., Pitkänen, I., Rönkkömäki, H., Perämäki, P. (1998) Thermal and infrared spectroscopic characterization of historical mortars. *Thermochimica Acta*, Vol. 320, No. 1–2, pp. 127-133.

Pagnotta, S., Lezzerini, M., Ripoll-Seguer, L., Hidalgo, M., Grifoni, E., Legnaioli, S., Lorenzetti, G., Poggialini, F., Palleschi, F. (2017) Micro-Laser-Induced Breakdown Spectroscopy (Micro-LIBS) Study on Ancient Roman Mortars. *Applied Spectroscopy*, Vol. 71, No. 4, pp. 721–727.

Pavía, S., Caro, S. (2008) An investigation of Roman mortar technology through the petrographic analysis of archaeological material. *Construction and Building Materials*, Vol. 22, No. 8, pp. 1807-1811.

Raneri, S., Barone, G., Lezzerini, M., Mazzoleni, P., Neri F.N. (2017) Mapping building materials and alteration forms to diagnosis, conservation and restore: a Norman castle in Sicily. In *Proceedings of Defensive Architecture of the Mediterranean. XV to XVIII centuries*, Vol. V, Echarri Iribarren (Ed.), Editorial Universitat Politècnica de Valencia.

Spizzichino, V., Fantoni, R. (2014) Laser Induced Breakdown Spectroscopy in Archaeometry: A Review of Its Application and Future Perspectives. *Spectrochimica Acta Part B: Atomic Spectroscopy*, Vol. 99, pp. 201–209.

Tognoni, E., Palleschi, V., Corsi, M., Cristoforetti, G. (2002). Quantitative micro-analysis by laser-induced breakdown spectroscopy: a review of the experimental approaches. *Spectrochimica Acta Part B: Atomic Spectroscopy*, Vol. 57, No. 7, pp. 1115–1130.

Velosa, A.L., Coroado, J., Veiga, M.R., Rocha, F. (2007) Characterisation of roman mortars from Conímbriga with respect to their repair. *Materials Characterization*, Vol. 58, No. 11–12, pp. 1208-1216.

Walker, R., Pavía, S. (2011) Physical properties and reactivity of pozzolans, and their influence on the properties of lime–pozzolan pastes. *Materials and Structures*, Vol. 44, No. 6, pp. 1139–1150.

Wilsch, G., Weritz, F., Schaurich, D., Wiggenhauser, H. (2005) Determination of chloride content in concrete structures with laser-induced breakdown spectroscopy. *Construction and Building Materials*, Vol. 19, No. 10, pp. 724-730.

Wold, S., Esbensen, K., Geladi, P. (1987). Principal component analysis. *Chemometrics and Intelligent Laboratory Systems*, Vol. 2, No. 1–3, pp. 37–52.

Yaseen, I.A.B., Al-Amoush, H., Al-Farajat, M., Mayyas, A. (2013) Petrography and mineralogy of Roman mortars from buildings of the ancient city of Jerash, Jordan. *Construction and Building Materials*, Vol. 38, pp. 465-471.